Anand et al., http://www.jcb.org/cgi/content/full/jcb.201308006/DC1

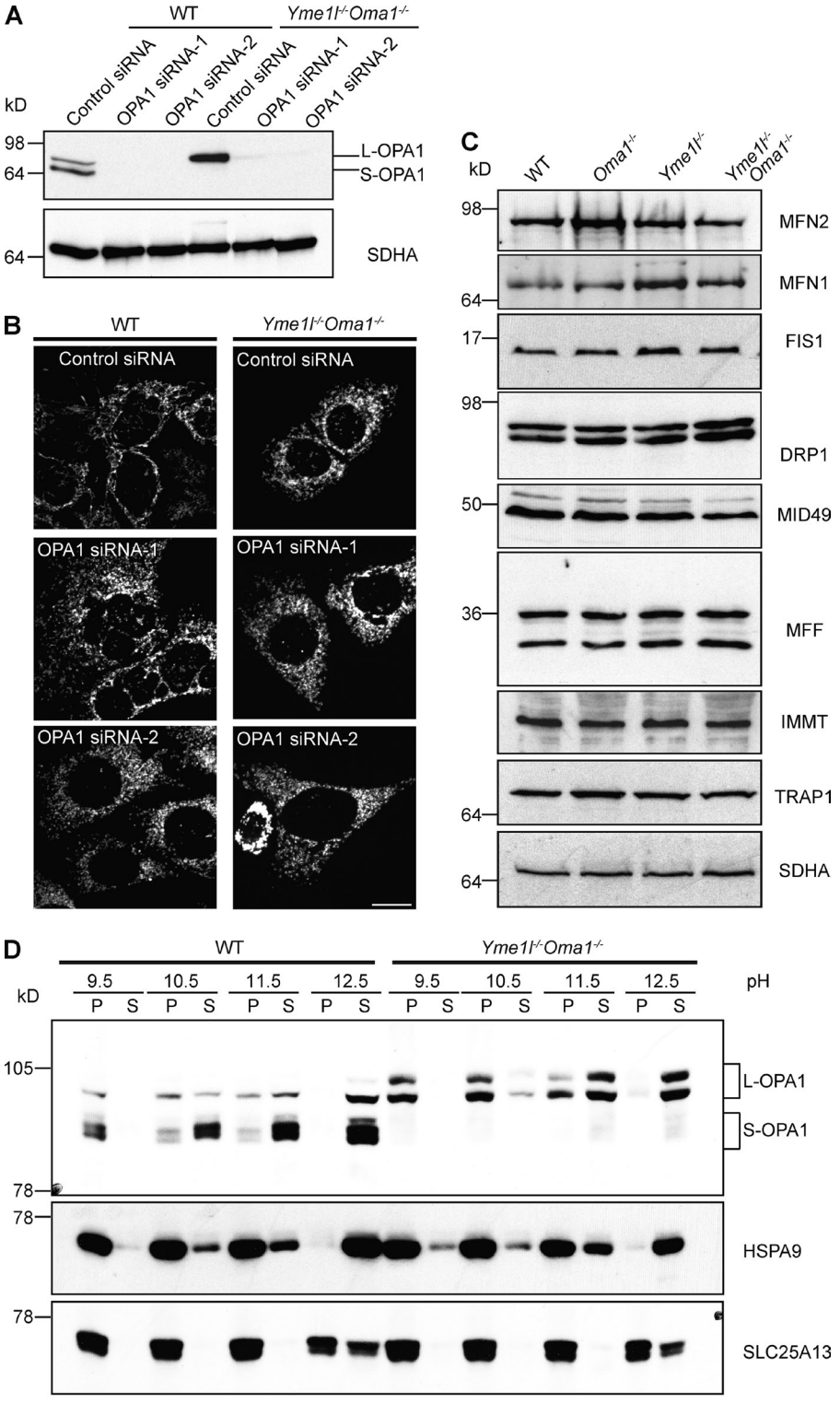

Figure S1. **The formation of tubular mitochondria in *Yme1l*$^{-/-}$*Oma1*$^{-/-}$ cells depends on OPA1.** (A) Immunoblot analysis of lysates of WT and *Yme1l*$^{-/-}$*Oma1*$^{-/-}$ MEFs after siRNA-mediated down-regulation of OPA1. Two independent siRNA oligos targeting *Opa1* were used (siRNA-1 and siRNA-2). (B) Depletion of OPA1 causes mitochondrial fragmentation in WT and *Yme1l*$^{-/-}$*Oma1*$^{-/-}$ MEFs. Bar, 15 µm. (C) Immunoblot analysis of cell lysates of WT, *Oma1*$^{-/-}$, *Yme1l*$^{-/-}$, and *Yme1l*$^{-/-}$*Oma1*$^{-/-}$ MEFs using antibodies against MFN2 (anti–rabbit; Sigma-Aldrich), MFN1 (anti–rabbit; Abcam), FIS1 (anti–rabbit; Proteintech), DRP1 (anti–mouse; BD), MID49 (anti–rabbit; Proteintech), IMMT (anti–rabbit; Proteintech), TRAP1 (anti–mouse; BD), and SDHA (anti–mouse; Invitrogen). (D) Alkaline extraction of mitochondria from WT and *Yme1l*$^{-/-}$*Oma1*$^{-/-}$ MEFs at the indicated pHs demonstrating differential solubility of L- and S-OPA1. The mitochondrial Hsp70 protein HSPA9 is soluble in the matrix, whereas the mitochondrial carrier protein SLC25A13 (CITRIN) is an integral IM protein.

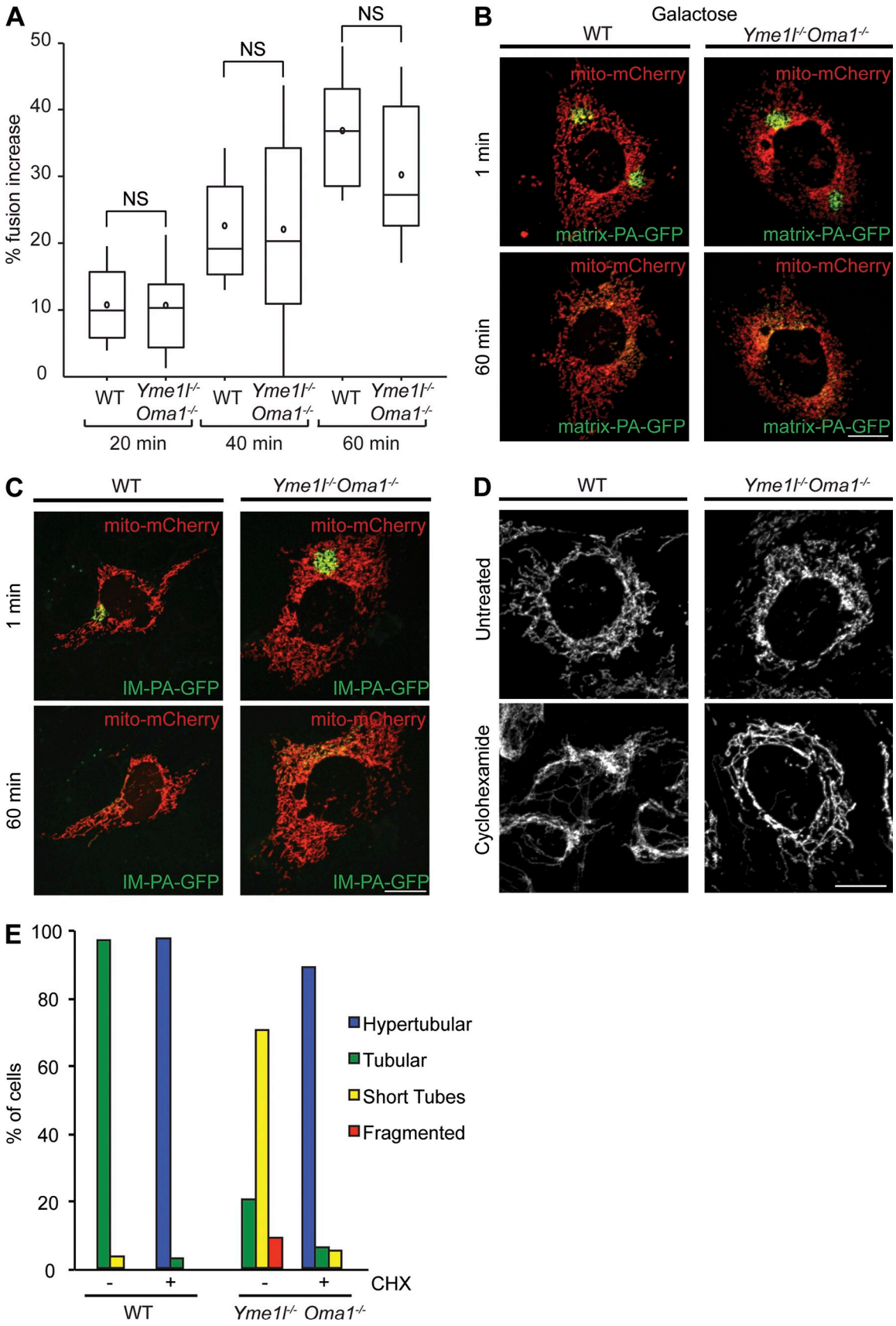

Figure S2. **Mitochondrial fusion in *Yme1l*$^{-/-}$*Oma1*$^{-/-}$ cells.** (A) PA-GFP targeted to the matrix was used to monitor fusion by the time-dependent dilution and redistribution of GFP fluorescence in WT and *Yme1l*$^{-/-}$*Oma1*$^{-/-}$ MEFs grown in glucose-containing media. Results are shown as a box plot representation of mitochondrial fusion quantified at 20, 40, or 60 min after photoactivation (WT vs. *Yme1l*$^{-/-}$*Oma1*$^{-/-}$ cells; P = 0.91 at 20 min, P = 0.91 at 40 min, and P = 0.14 at 60 min). (B) Mitochondrial fusion occurs in WT and *Yme1l*$^{-/-}$*Oma1*$^{-/-}$ MEFs grown in galactose-containing media for 24 h. (C) PA-GFP targeted to the IM (IM-PA-GFP; amino-terminal region of ABCB10 fused to mito-mCherry) was expressed in WT and *Yme1l*$^{-/-}$*Oma1*$^{-/-}$ MEFs, and fusion was monitored. (D) Mitochondria hyperfuse in *Yme1l*$^{-/-}$*Oma1*$^{-/-}$ cells under stress. *Yme1l*$^{-/-}$*Oma1*$^{-/-}$ cells were incubated for 8 h in the presence of 10 μM cycloheximide. Bars, 15 μm. (E) Quantification of mitochondrial morphology ($n \geq 100$).

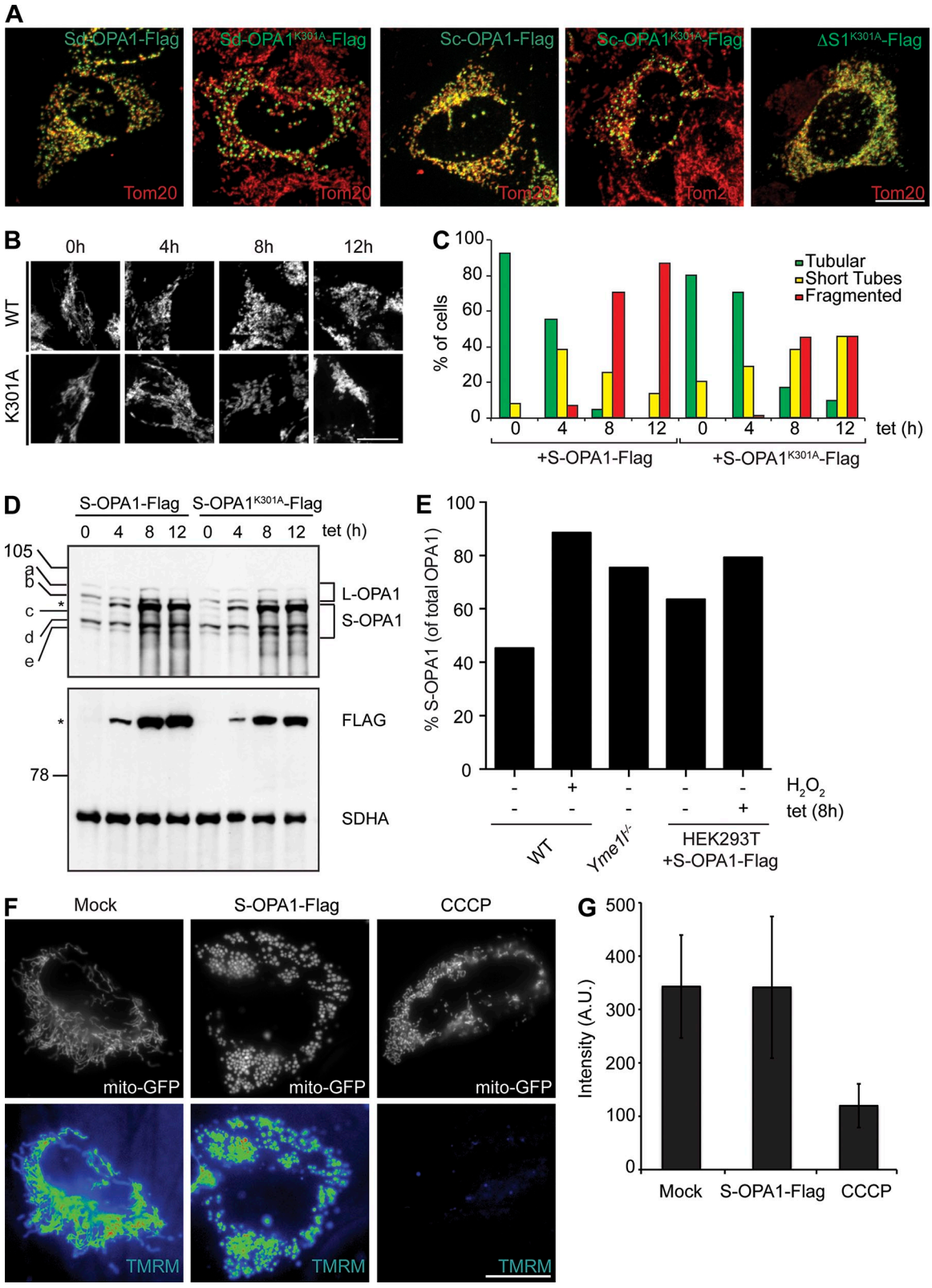

Figure S3. **Ectopic S-OPA1 expression induces mitochondrial fragmentation but does not cause general mitochondrial dysfunction.** (A) WT MEFs overexpressing human S-OPA1 form d (Sd-OPA1-Flag; amino acids 1–97 of rat AIF fused to amino acids 210–997 of human OPA1 sp7) and human S-OPA1 form c (Sc-OPA1; amino acids 1–97 of rat AIF fused to amino acids 194–997 of human OPA1 sp7) fragment mitochondria, whereas Sd-OPA1^{K301A} and Sc-OPA1^{K301A} variants form punctae. Noncleavable L-OPA1^{K301A} (ΔS1^{K301A}-Flag) expression neither fragments the mitochondrial network nor accumulates in punctae structures. Bar, 15 µm. (B) Tetracycline-induced, stable expression of rat S-OPA1-Flag (amino acids 1–97 of rat AIF fused to amino acids 230–997 of rat OPA1) and rat S-OPA1^{K301A}-Flag in HEK293T cells. Mitochondrial morphology was assessed at the indicated time points after the addition of tetracycline. (C) Quantification of mitochondrial morphology in cells shown in B (n > 100). (D) Immunoblot analysis of cell lysates using anti-OPA1, anti-Flag, and anti-SDHA antibodies. The asterisks denote tetracycline-induced rat S-OPA1-Flag. (E) The induced increase in S-OPA1 levels is associated with mitochondrial fragmentation in different cells. After SDS-PAGE and immunoblotting, S-OPA1 forms were quantified by laser densitometry (from Figs. 3 B and S3 D) and are shown as the percentage of total OPA1. (F) Transient overexpression of rat S-OPA1-Flag does not impair the mitochondrial membrane potential monitored by TMRM fluorescence. For control, mitochondria were depolarized by the addition of 20 µM CCCP for 30 min. (G) Quantification of TMRM intensity in mock-treated, S-OPA1–expressing, and CCCP-treated cells.